Autler-Townes Splitting in Molecular Lithium: Prospects for All-Optical Alignment of Nonpolar Molecules

Jianbing Qi,[1] Guenadiy Lazarov,[1] Xuejun Wang,[1] Li Li,[2] Lorenzo M. Narducci,[3] A. Marjatta Lyyra,[1] and Frank C. Spano[4]

[1]*Department of Physics, Temple University, Philadelphia, Pennsylvania 19122*
[2]*Department of Modern and Applied Physics, Tsinghua University, Beijing, China 10084*
[3]*Department of Physics, Drexel University, Philadelphia, Pennsylvania 19104*
[4]*Department of Chemistry, Temple University, Philadelphia, Pennsylvania 19122*

(Received 17 February 1999)

We demonstrate Autler-Townes (AT) splitting in molecular lithium using cw triple resonance spectroscopy. The pump and tunable probe lasers create sub-Doppler double resonance excitation of an upper rovibrational level. The line shape is split in the presence of a third, coupling laser. The AT line shape consists of the superposition of several narrower twin peaks, one for each $|M_J|$. The splitting is proportional to $|M_J|$ enabling resolution of the individual M_J peaks. Thus, this all-optical technique can be used to align nonpolar molecules. The line shapes are in excellent agreement with theory.

PACS numbers: 33.40.+f, 42.50.Hz

Continuous wave (cw) triple resonance spectroscopy provides an effective tool for selective control and transfer of population in quantum states of atoms and molecules [1,2]. In diatomic molecules rovibrational selectivity can be achieved automatically using this technique because the rotational and vibrational levels are spectrally resolvable. In this paper we show how to extend the degree of state selectivity of this approach to the degenerate magnetic sublevels using the Autler-Townes (AT) splitting induced by one of the lasers. We thus demonstrate an all-optical method of attaining molecular alignment, one of the most important goals in modern reaction dynamics. An all-optical method has advantages over techniques based on dc fields [3–5] because of its ability to align nonpolar molecules.

The ac Stark effect and AT splitting in gas-phase molecules have only recently been investigated. Previous experiments [6–10] used pulsed laser excitation to overcome Doppler broadening and wavelength limitations imposed by cw lasers. Light shifts in the two-photon excitation spectra of CO and NO were reported by Girard *et al.* [6] and by Huo *et al.* [7], respectively. Quesada *et al.* measured AT splitting in H_2 [8]. The ac Stark effect in the (2 + 2) resonance-enhanced multiphoton ionization (REMPI) of N_2 and two-photon laser-induced fluorescence of CO were measured by Girard *et al.* [9]. Using a two-color scheme Xu *et al.* [10] measured the ac Stark shift and AT splitting in the (2 + 2) REMPI spectrum of CO. In what follows we present what we believe is the first measurement of sub-Doppler on-resonance AT splitting in a molecular gas using cw lasers. In this manner we can avoid multiphoton ionization inherent to pulsed excitation.

We report the AT splitting in the $G\,^1\Pi_g$ excited state of $^7Li_2$. The experimental setup has been described previously [1]. Lithium dimers are generated in a five-arm stainless steel heat pipe with operating temperature around 1000 K and with the argon buffer gas pressure in the 100–200 mTorr range. Three Coherent 699-29 dye lasers (0.5 MHz bandwidth) are arranged so that the pump laser, L1, and coupling laser, L3, are copropagating while the probe laser, L2, is counterpropagating with respect to L1 and L3. All three laser beams are aligned coaxially, and are linearly polarized in a common direction. In this experiment, the pump laser L1 is modulated by an optical chopper. The modulated fluorescence signals are detected by a photomultiplier tube (PMT) at the side arm of the oven for total fluorescence detection, and by a spectrometer (SPEX 1404)/cooled PMT for single channel fluorescence detection. In the former case, violet/UV bandpass filters are used to facilitate detection of the violet side fluorescence outside the range of the individual laser wavelengths [1]. The PMT signal is fed to a lock-in amplifier with a 300 msec time constant. The probe is scanned in steps of 1 MHz with a typical 1 GHz scan taking five minutes. At each step the lock-in output is sampled 500 times. All laser frequencies are determined by using standard iodine calibration.

The relevant energy levels in our experiment are shown in Fig. 1. The $G\,^1\Pi_g$ level is prepared by sub-Doppler optical-optical double resonance (OODR) excitation. The pump laser L1 excites a molecule from the ground state $X\,^1\Sigma_g^+$ $(\nu = 2, J = 11)$ to a selected intermediate level $A\,^1\Sigma_u^+$ $(\nu = 10, J = 12)$. The probe laser L2 further excites the molecule to the upper level $G\,^1\Pi_g$ $(\nu = 12, J = 12, f$ parity). Through collisional energy transfer, population in the upper level is transferred to nearby triplet states, which then decay to lower triplet states. The resulting violet/UV radiation is detected. The coupling laser L3 couples the upper level to a second intermediate level $A\,^1\Sigma_u^+$ $(\nu = 14, J = 12)$ (see Fig. 1). The pump and probe lasers are focused inside the heat pipe to spot sizes

 0031-9007/99/83(2)/288(4)$15.00

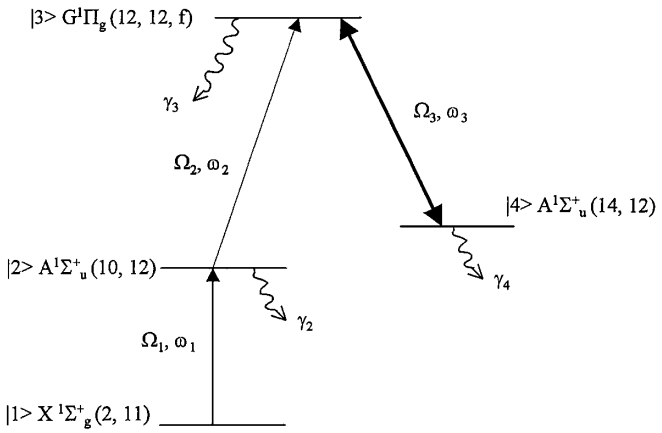

FIG. 1. Energy level diagram. The transition frequencies $\omega_{21}/2\pi c$, $\omega_{32}/2\pi c$, and $\omega_{34}/2\pi c$ are 15 667.033 cm^{-1}, 17 898.235 cm^{-1}, and 17 033.544 cm^{-1}, respectively.

of 360 and 220 μm, respectively. Their powers are kept below 10 mW in order to minimize power broadening. The much stronger coupling laser, whose power varies in the range from 100–300 mW, is focused to a spot size of 450 μm. The larger spot size of L3 is chosen to enhance the spatial uniformity of the coupling laser field for those molecules near the center of the beams. These molecules experience the strongest pump and probe excitation and, therefore, contribute the bulk of the signal.

In our experiments the pump laser is held on resonance. With the coupling laser off, scanning the probe laser while monitoring the upper level fluorescence leads to the usual OODR spectrum for the $G\,^1\Pi_g$ level shown in Fig. 2(a). When the same experiment is repeated with the coupling laser L3 on, the OODR signal splits into two symmetric peaks. Figures 2(b)–2(d) show the spectra corresponding to three different values of the coupling laser power. The peaks are significantly diminished in height relative to the OODR peak and are several times broader.

In order to understand the nature of the AT line shapes, we solved the density matrix equations of motion for a four level system interacting with pump, probe, and coupling lasers [11] (see Fig. 1). The pump and probe are treated perturbatively and the coupling field exactly. Each laser is assumed (near) resonant with a single rovibronic transition. Fluorescence is observed near the beam waists of all three lasers, with the detected fluorescence coming from a segment of the interaction region much shorter than the Rayleigh range. Hence, the linearly polarized electric fields can be approximated by

$$E_i(\vec{r},t) = E_i\vec{\varepsilon}\exp[-(r/w_i)^2]\cos(k_i z - \omega_i t)\,,$$

where w_i, k_i, and ω_i denote the spot size at the beam waist, the wave number, and the frequency of the ith laser, respectively, and $\vec{\varepsilon}$ is the unit polarization vector. Under steady state conditions, the upper level population for a molecule with orientation M, radial position r relative to the common axis of the three laser beams, and velocity ν_z is given by

$$\rho_{33}^{M}(r,\nu_z) = \frac{\Omega_{1,M}^2(r)\Omega_{2,M}^2(r)}{A\gamma_3[(k_1\nu_z)^2+\gamma_{12}^2]} \times \mathrm{Im}\left\{\frac{[\Delta_2-\Delta_3+(k_1+k_2-k_3)\nu_z - i\gamma_{14}] - \frac{\gamma_4\Omega_{3,M}^2(r)\,(\Delta_3+k_3\nu_z-i\gamma_{34})}{2\Omega_{3,M}^2(r)\gamma_{34}+\gamma_4[(\Delta_3+k_3\nu_z)^2+\gamma_{34}^2]}}{[\Delta_2+(k_1+k_2)\nu_z - i\gamma_{13}][\Delta_2-\Delta_3+(k_1+k_2-k_3)\nu_z - i\gamma_{14}] - \Omega_{3,M}^2(r)} + \frac{2\gamma_{12}^C}{\gamma_2}\,\frac{\Delta_2-\Delta_3+(k_2-k_3)\nu_z - i\gamma_{24} - \frac{\gamma_4\Omega_{3,M}^2(r)\,(\Delta_3+k_3\nu_z-i\gamma_{34})}{2\Omega_{3,M}^2(r)\gamma_{34}+\gamma_4[(\Delta_3+k_3\nu_z)^2+\gamma_{34}^2]}}{(\Delta_2+k_2\nu_z - i\gamma_{23})[\Delta_2-\Delta_3+(k_2-k_3)\nu_z - i\gamma_{24}] - \Omega_{3,M}^2(r)}\right\} \quad (1)$$

with

$$A = 1 - \frac{\Gamma_{34}}{\gamma_3} + \frac{\gamma_4}{\gamma_3}\,\frac{2\Omega_{3,M}^2\gamma_{34}+\Gamma_{34}[(\Delta_3+k_3\nu_z)^2+\gamma_{34}^2]}{2\Omega_{3,M}^2\gamma_{34}+\gamma_4[(\Delta_3+k_3\nu_z)^2+\gamma_{34}^2]}\,.$$

The detunings of the probe and coupling lasers from the molecular transition frequencies ω_{ij} are $\Delta_2 \equiv \omega_{32} - \omega_2$ and $\Delta_3 \equiv \omega_{34} - \omega_3$, respectively. The Rabi frequencies of all three lasers depend on both the molecule's orientation as well as its distance from the beam axis. When the ith laser is tuned near resonance with the i, $i+1$ transition, the Rabi frequency is given by $\Omega_{i,M}(r) \equiv (\mu_{i,i+1}^M E_i/2\hbar)\exp[-(r/w_i)^2]$, where $\mu_{i,i+1}^M$ is the M-dependent transition dipole moment between levels i and $i+1$ [12]. In Eq. (1) γ_i is the damping rate of the ith level, including radiative as well as collisional contributions. The decay rate of the coherence between levels i and j ($\neq i$) is $\gamma_{ij} = (\gamma_i+\gamma_j)/2 + \gamma_{ij}^c$, where γ_{ij}^c is the pure dephasing contribution induced by phase interrupting collisions. Γ_{34} is the damping rate of the upper level to the intermediate level, $A\,^1\Sigma_u^+$ ($\nu = 14, J = 12$).

If the collisional population transfer from the upper level to the nearby fluorescent triplet state is independent of M, the signal is obtained from Eq. (1) by summing over M and averaging over the Doppler and transverse laser profiles. The final result is

$$S(\Delta_2) = \sum_M \int_0^\infty r\,dr\langle\rho_{33}^M(r,\nu_z)\rangle_D\,, \quad (2)$$

where $\langle\cdots\rangle_D$ indicates the Doppler average. We take the linewidth of the Doppler profile to be much greater than the homogeneous linewidth.

In deriving Eq. (1) we assume that the pump laser is tuned to the center of the Doppler broadened line

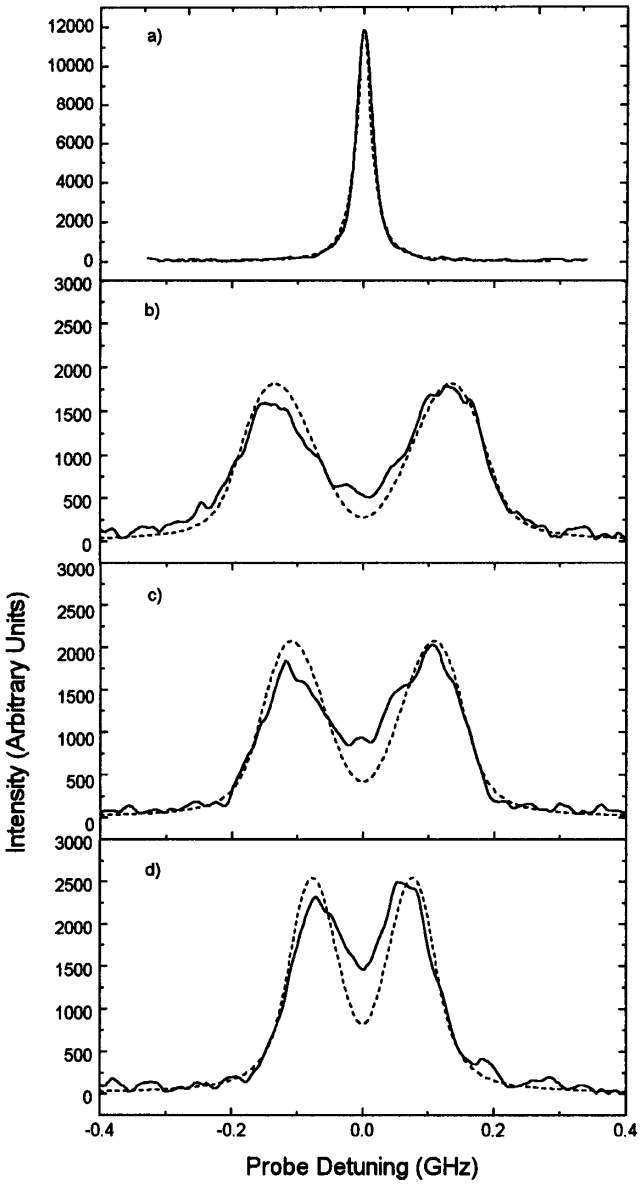

FIG. 2. Violet/UV fluorescence from the $G\,^1\Pi_g$ $(\nu = 12, J = 12, f)$ level as a function of the probe detuning. (a) OODR spectrum with the coupling field off. (b)–(d): AT spectra for a resonant coupling field with a power of 300 mW (b), 200 mW (c), and 100 mW (d). The solid lines indicate experimental spectra while the dashed lines are theoretical simulations based on Eq. (2).

transition, and neglect the time dependence caused by the transverse motion of the molecules, which is expected to yield negligible corrections. In addition, we invoke the simplifying relationship $\gamma_{ij}^c = \gamma_{i1}^c + \gamma_{j1}^c$ $(i, j \neq 1)$. This eliminates a small interference term which would appear on the right-hand side of (1) [13,14]. The first and second terms in Eq. (1) represent coherent and incoherent contributions, respectively. When the coupling field is off, Eq. (1) reduces to a form similar to the atomic OODR line shape expression derived in Ref. [14]. The coherent term contains Doppler-free resonances when $k_2 \approx -k_1$. The incoherent term depends on phase interrupting collisions and contains residual Doppler broadening. When the coupling field is on, the denominators of both terms in Eq. (1) contain two poles which give rise to the two peaks in the AT spectrum. When the coupling field is on resonance ($\Delta_3 = 0$) and $\Omega_{3,M}(r)$ is much greater than any of the relaxation rates, the poles are located at $\pm\Omega_{3,M}$ for the molecules with orientation M. According to Eq. (2), the broadening of a given line within the AT split pair depends on the coupling field through the distribution of Rabi frequencies over M and r.

In order to compare with experiment we evaluate Eq. (2) using the experimental wave numbers $k_1 = 2\pi \times 15.6 \times 10^3\ \mathrm{cm}^{-1}$, $k_2 = -1.1k_1$ (neglecting the small change in k_2 as the probe is scanned) and $k_3 = 1.1k_1$; the spot sizes $w_1 = 360\ \mu$m, $w_2 = 220\ \mu$m, and $w_3 = 450\ \mu$m; and the appropriate M dependence for $\mu_{i,i+1}^M$ [12] assuming an R transition for the pump laser and Q transitions for both the probe and the coupling lasers. The intermediate level lifetime γ_2^{-1} $(\approx\gamma_4^{-1})$ is set to the experimentally determined value of 17 nsec, which includes an 18.8 nsec natural lifetime extrapolated to 17 nsec at 200 mTorr to include collisional redistribution [15]. Since information about the various dephasing rates in Li_2 is not available, we assume a simplified model where $\gamma_{i1}^c = \gamma^c$. We perform our calculations by first locating values of γ_3 and γ^c which, when inserted into Eqs. (1) and (2), best reproduce (i) the experimental OODR line shape in Fig. 2(a) when $E_3 = 0$, and (ii) the experimental AT spectrum for the highest coupling field power [Fig. 2(b)], with E_3 adjusted to reproduce the experimental AT splitting. We find that the splitting and broadening are mainly determined by E_3, but the ratio of the OODR peak intensity to the AT peak intensity is sensitive to the choice of γ_3 and γ^c. The values $\gamma^c = 32$ MHz and $\gamma_3 = 2\gamma_2$ give the dashed curves in Figs. 2(a) and 2(b). Calculations at lower coupling field powers [dashed curves in Figs. 2(c) and 2(d)] are conducted without any additional parameter changes or renormalizations.

Figure 2 shows the theoretical AT line shapes to be in excellent agreement with experiment. We have verified that, as in the atomic case, the AT splitting is linearly proportional to the magnitude of the coupling field. However, in the molecular case the broadening of the AT line shape reflects the distribution of orientation dependent Rabi frequencies. The broad twin peaks in Figs. 2(b)–2(d) are due to a superposition of eleven narrow twin peaks, one for each nonzero value of $|M|$ for $J = 12$ except $|M| = J$, since these states are not excited in the $R(11)$ pump transition. The splitting for each set is approximately given by $2\Omega_{3,M}(r = 0)/2\pi$. Inserting the transition dipole moment factors into the Rabi frequency gives

$$2\Omega_{3,M}(0)/2\pi \approx [|M|/\sqrt{2J(J+1)}]\mu_e|\langle\nu\,|\,\nu'\rangle|E_3/h\,, \tag{3}$$

where the linearity in $|M|$ derives from the rotational selection rule for a Q transition. In Eq. (3), μ_e is the

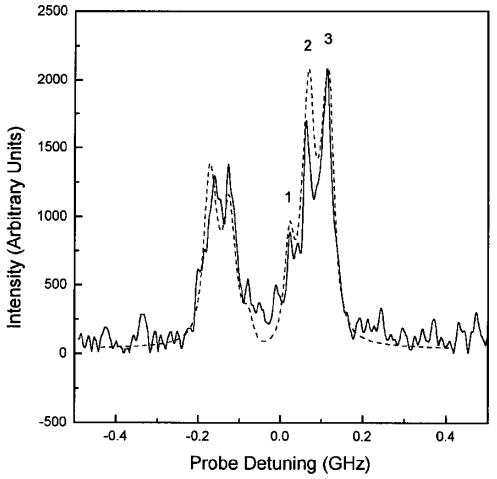

FIG. 3. The AT spectrum of the $G\,^1\Pi_g$ $(\nu = 12, J = 3, f)$ level taken using single channel detection. The coupling laser is slightly detuned with a power of 300 mW. The peaks are labeled according to the value of $|M|$. The solid lines indicate experimental spectra while the dashed lines are theoretical simulations based on Eq. (2). The transition frequencies $\omega_{21}/2\pi c$, $\omega_{32}/2\pi c$, and $\omega_{34}/2\pi c$ are 15 709.321 cm^{-1}, 17 904.349 cm^{-1}, and 17 036.686 cm^{-1}, respectively.

electronic dipole moment oriented perpendicular to the molecular axis as for a $^1\Sigma \leftrightarrow {}^1\Pi$ transition and $|\langle \nu \,|\, \nu' \rangle|^2$ is the Franck-Condon (FC) factor. Our calculations show that the individual magnetic sublevel lines are approximately 10–15 MHz broader than the OODR line due to the variation of the Rabi frequency over the Gaussian transverse profile. The peak of the composite AT line shape coincides with that for the $|M| = 8$ component. Hence, for the $Q(12)$ transition the overall AT splitting from Eq. (3) is $\Delta_{\text{AT}} \approx 0.45\mu_e|\langle \nu \,|\, \nu' \rangle|E_3/h$, from which we determine $\mu_e = 3.4$ a.u. using the calculated FC factor of 0.27 and the experimental splitting and field intensity from Fig. 2(b). For high coupling field powers (>100 mW for $w_3 = 450$ μm), the FWHM of either of the composite AT peaks is approximately linearly proportional to the coupling field.

According to Eq. (3), it should be possible to resolve the individual $|M|$ components in the AT spectrum for lower J values. We have, in fact, observed the AT splitting for a level with $J = 3$, starting from a ground state $J = 4$ level with the rotational transitions $P(4)$, $Q(3)$, and $Q(3)$ excited by the pump, probe, and coupling lasers, respectively. There are then only three sets of twin peaks corresponding to $|M| = 1$, 2, and 3. Figure 3 shows the experimental spectrum as well as the theoretical spectrum from Eq. (2). The $|M| = 2$ and 3 peaks are partially resolved, whereas the $|M| = 1$ peak falls below the noise level. The signal to noise ratio is reduced by about a factor of 3 compared to the (ground state) $J = 11$ spectra primarily because of the lower thermal population of the $J = 4$ level compared to the $J = 11$ level. Noise is due to laser intensity fluctuations and frequency drift as well as the PMT dark current. To obtain the rather good agreement between theory and experiment the parameter γ^c is set to $\gamma^c = 10$ MHz with all others unchanged from the $J = 11$ case. The slight asymmetry of the peaks is due to detuning of the coupling field. (The off-resonance AT line shape will be considered in detail in a forthcoming paper.) In the simulation we take $\Delta_3 = 37$ MHz which is within the uncertainty of the wave meter reading.

In summary, we have observed magnetic sublevel resolved molecular AT splitting in a Doppler broadened sample. Tuning the probe to the $|M|$th magnetic sublevel peak prepares aligned excited molecules which are predominantly in the states $\pm M$. We expect to achieve even greater spectral resolution (and hence better alignment) by using a well-collimated molecular beam. This will eliminate the residual Doppler broadening which resides in the AT spectrum [see Eq. (1)] as well as the collisional dephasing contribution to the linewidth. Our novel all-optical alignment technique should be useful, for example, in crossed molecular beam experiments probing reaction dynamics.

We are grateful to J. Huennekens, R. W. Field, E. Arimondo, H. Ling, and R. Gordon for valuable discussions, and to J. Magnes for technical assistance. This work was supported by the NSF. One of us (L. L.) was supported by the NNSF of China.

[1] A. M. Lyyra, H. Wang, T. J. Whang, and W. C. Stwalley, Phys. Rev. Lett. **66**, 2724 (1991).
[2] J. Martin, B. W. Shore, and K. Bergmann, Phys. Rev. A **54**, 1556 (1996).
[3] B. Friedrich, A. Slenczka, and D. R. Herschbach, Chem. Phys. Lett. **221**, 333 (1994).
[4] H. J. Loesch and J. Remscheid, J. Chem. Phys. **93**, 4779 (1990).
[5] M. Wu, R. J. Bemish, and R. E. Miller, J. Chem. Phys. **101**, 9447 (1994).
[6] B. Girard, N. Billy, J. Vigue, and J. C. Lehmann, Chem. Phys. Lett. **102**, 168 (1983).
[7] W. M. Huo, K. P. Gross, and R. L. McKenzie, Phys. Rev. Lett. **54**, 1012 (1985).
[8] M. A. Quesada, A. M. F. Lau, D. H. Parker, and D. W. Chandler, Phys. Rev. A **36**, 4107 (1987).
[9] B. Girard, G. O. Sitz, R. N. Zare, N. Billy, and J. Vigue, J. Chem. Phys. **97**, 26 (1992).
[10] S. Xu, G. Sha, B. Jiang, W. Sun, X. Chen, and C. Zhang, J. Chem. Phys. **100**, 6122 (1994).
[11] S. Stenholm, *Foundations of Laser Spectroscopy* (Wiley Interscience, New York, 1984).
[12] W. Demtroder, *Laser Spectroscopy* (Springer-Verlag, Berlin, 1982).
[13] M. J. O'Callaghan and A. Gallagher, Phys. Rev. A **39**, 6190 (1989).
[14] M. J. O'Callaghan and J. Cooper, Phys. Rev. A **39**, 6206 (1989).
[15] G. Baumgartner, H. Kornmeier, and W. Preuss, Chem. Phys. Lett. **107**, 13 (1984).